Volume 9, Issue 6, 2019, 4502 - 4516 ISSN 2069-5837
Biointerface Research in Applied Chemistry
www.BiointerfaceResearch.com
https://doi.org/10.33263/BRIAC96.502516
Original Research Article Open Access Journal
Received: 13.08.2019 / Revised: 12.10.2019 / Accepted: 16.10.2019 / Published on-line: 21.10.2019

Structural and vibrational studies of equilenin, equilin and estrone steroids

Silvia Antonia Brandán [1, *]
[1]Cátedra de Química General, Instituto de Química Inorgánica, Facultad de Bioquímica. Química y Farmacia, Universidad Nacional de Tucumán, Ayacucho 471, (4000) San Miguel de Tucumán, Tucumán, Argentina
*corresponding author e-mail address: ***sbrandan@fbqf.unt.edu.ar*** | Scopus ID 6602262428

ABSTRACT
Three species associated with estrogens have been studied in this work, equilenin, equilin and estrone. Their molecular structures have been theoretically studied in gas phase with the hybrid B3LYP/6-31G* method. NBO, AIM and frontier orbital calculations were computed for the three species at the same level of theory. Higher dipole moment and volume were observed for estrone while equilin presents higher volume than equilenin but lower dipole moment value. Probably, the unsaturated C=C in the B ring of equilin could explain those differences. The differences observed in the properties could be clearly explained by differences in the dihedral angles. The analyses of MK and Mulliken charges evidence the higher variations on the C atoms common to the B, C and D rings in the three species. The mapped MEP surfaces show that both A and B rings of equilenin are different from the other ones because they have aromatic naphthalene core, as was evidenced experimentally. The NBO studies support the higher stability of equilin, in relation to equilenin and estrone while the AIM analyses reveal the higher stability for estrone. The gap values suggest that equilenin is the most reactive species due to its higher global electrophilicity value, in agreement with the higher stability observed for this species while the higher global nucleophilicty values are observed for equilin and estrone. Here, the harmonic force fields, scaled force constants and the complete assignments of 108, 114 and 120 vibration modes for equilenin, equilin and estrone, respectively are reported for first time.
Keywords: *Steroids; Force fields; Vibrational analysis; DFT calculations; Molecular structure.*

1. INTRODUCTION
Steroid hormones are important compounds found in the human body that are derived from cholesterol and have characteristics lipid-soluble and normally are grouped into two classes: corticosteroids and sex steroids differenced by bonding receptors and biological functions [1-17]. Hence, different factors (solubilization, motility, transport, metabolism, and complementarity of fit between hormone and receptor) have influence on the activity of steroid hormones. Thus, according to the receptors to which they bind there are five types: gluco-corticoids, mineralo-corticoids, androgens, estrogens, and progesterone. Steroid hormones have multiple functions in the human body being among others, control metabolism, immune functions, inflammation, salt and water balance, development of sexual characteristics, and the ability to resist illness and hurt [18-22]. For instance, estrone, estradiol, estriol, equilenin, equilin and their derivatives are some of species associated with estrogens and, obviously, to steroid hormones [1-9,11,13]. Structural studies on these hormones and their quick identifications are very important from medicinal, chemistry, human health, environmental and pharmacological points of view because when these hormones are discharged toward the environmental can affect the systems of all living beings [14,15]. On the other hand, from long time the vibrational spectroscopy was a very useful technique used widely to detect the species related to steroid hormones, as evidenced in the numerous research papers published in the literature [10,12,14,17]. Hence, the knowledge of their structures is necessary to perform the complete and reliable vibrational assignments of these species. So far, previous vibrational works on those steroids were carried out without considering the corresponding force fields necessary to produce a correct assignment of all the bands observed in the infrared and Raman spectra [10,12,14,17]. These potential energy contributions are necessary to perform the vibrational assignments because, specifically, in the region of smaller wavenumbers region the vibration modes are strongly coupled with each other. In this study, the experimental available infrared and Raman spectra of equilenin, equilin and estrone steroids were completely assigned taking into account their corresponding harmonic SQM force fields by using the SQMFF methodology, the normal internal coordinates and the Molvib program [23-25]. A scheme of three structures studied in this work can be seen in **Scheme 1** together with the definitions of four rings.

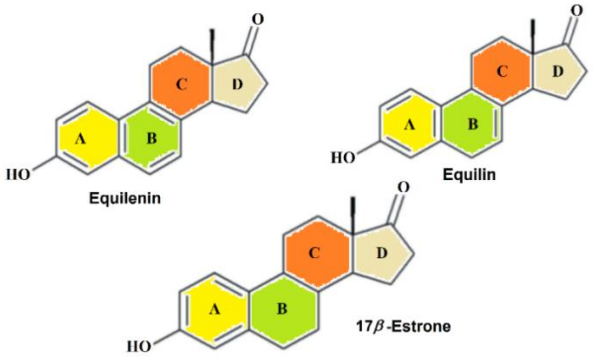

Scheme 1. Structure of equilenin, equilin and estrone steroids with definitions of rings.

Hence, the harmonic force fields of equilenin, equilin and estrone steroids species in gas phase were obtained first optimizing the three structures with the hybrid B3LYP/6-31G* method [26,27] and, then, their corresponding vibrational spectra were predicted in order to compare with the experimental ones. In additional form, the harmonic force constant for the three species was also reported together with the studies of frontier orbitals because the

predictions of the reactivities and behaviours of three species are of interest taking into account their important biological functions. The knowledge of structural properties could explain their biological activities or mechanisms of action of steroid hormones.

2. MATERIALS AND METHODS

The initial theoretical structure of equilenin was that experimental determined by X-ray diffraction to 100 K by Frampton and MacNicol [13] and, later with this structure were modelled the structures corresponding to equilin and estrone by using the *GaussView* program [28]. The optimizations of three structures in gas phase were carried out with the Revision A.02 of Gaussian program [29] and by using the hybrid B3LYP/6-31G* method [26,27]. In **Figure 1** are presented the three structures with the atoms labeling and the definitions of four rings, as in scheme 1. The predicted energies values for the three species in gas phase were corrected by zero point vibrational energy (ZPVE) and the volumes in gas phase were computed at the same level of theory with the Moldraw program [30]. The scaled quantum mechanical force field (SQMFF) methodology together with the Molvib program was employed to obtain the harmonic force fields and the potential energy distribution (PED) contributions [23-25]. Here, the assignments oh three species were performed considering the corresponding normal internal coordinates, transferable scaling factors and only contributions ≥ 10%. In addition, the frontier orbitals and some remarkable descriptors were used to predict reactivities and behaviours of three species [31-41].

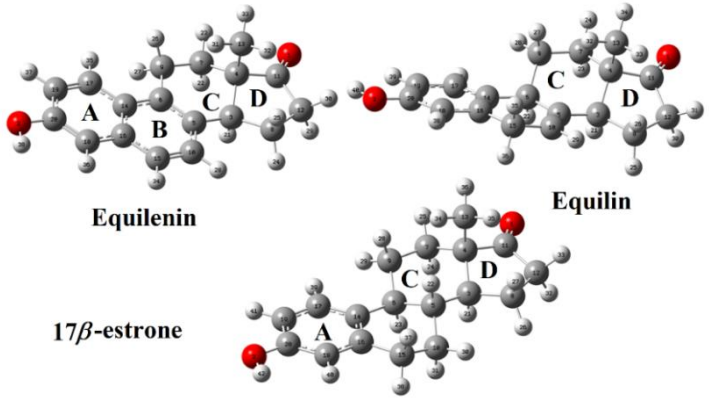

Figure 1. Molecular theoretical structures of equilenin, equilin and estrone steroids showing the definitions of rings.

The predicted Raman spectra in activities were converted to intensities for a better correlation with the experimental one [42,43]. Additional NBO and AIM calculations were performed to predict atomic charges and main delocalization energies [44-47].

3. RESULTS

Optimized Structures of all species in gas phase.

Structurally, equilenin [13] is different from equilin and estrogen in the B ring, as can be seen in **Figure 2**.

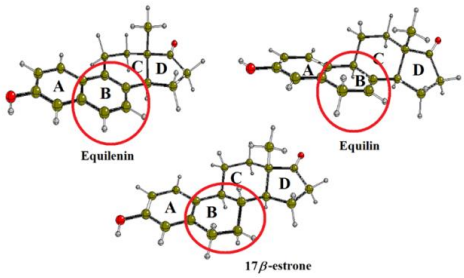

Figure 2. Theoretical structures of equilenin, equilin and estrone steroids showing in red circles the differences in the B rings.

Table 1. Calculated total energies (*E*) and by zero point vibrational energy (ZPVE), dipole moments (μ) and volumes (V) of equilenin, equilin and estrone in gas phase by using the B3LYP/6-31G* method.

B3LYP/6-31G* Method				
Species	E (Hartrees)	ZPVE (Hartrees)	μ (D)	V ($Å^3$)
Equinelin	-847.2153	-846.8965	3.34	291.3
Equilin	-848.3997	-848.0583	2.18	296.2
Estrone	-849.6227	-849.2569	3.80	304.0

Thus, in equilenin both A and B rings are practically coplanar forming a full aromatic naphthalene core, as mentioned by Frampton and MacNicol [13], with two aromatic C-H bonds in B. In equilin, due to the presence of a C=C in B only an aromatic C-H bond it is observed in this ring. On the contrary, in estrone there are two CH_2 groups in B, for which, the total number of atoms increase from 38 in equilenin to 42 in estrone while in equilin the total number of atoms is 40. Calculated total energies (*E*) and by zero point vibrational energy (ZPVE), dipole moments (μ) and volumes (V) of equilenin, equilin and estrone in gas phase by using the B3LYP/6-31G* method are presented in **Table 1**.

Apparently, the greater number of atoms in estrone justifies its higher dipole moment and volume values than the other two species. Moreover, the orientations, magnitudes and directions of dipole moment vectors in the three species are completely different, as evidenced in **Figure 3**.

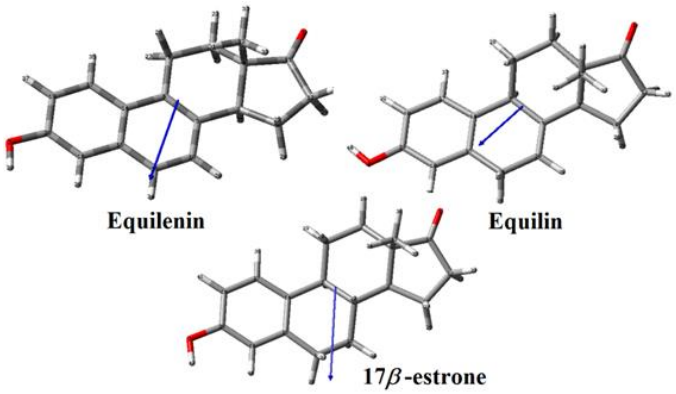

Figure 3. Orientations, magnitudes and directions of dipole moment vectors of equilenin, equilin and estrone steroids in gas phase by using the B3LYP/6-31G* method.

However, despite equilin presents higher volume than equilenin its dipole moment value is lower (2.18 D). This difference between equilenin and equilin probably could be explained by the presence

of the unsaturated C=C in B which rotates the C and D rings of the steroid generating the translation of the O1 atom belonging to C11=O1 group, as was experimentally observed for equilin by Sawicki et al [7]. This translation of the O1 atom was attributed by Sawicki et al [7] to the increased anti-human estrogenic 17β-hydroxysteroid dehydrogenase inhibitory behavior of equilin in relation to estrone. Furthermore, the methyl group in equilenin and equilin is also translated by 0.79 and 1.40 Å, respectively in relation to estrone increasing the estrogenic activity of equilenin than equilin [7].

Geometrical parameters in both media.

Here, the calculated geometrical parameters for equilenin, equilin and estrone steroids in gas phase by using the B3LYP/6-31G* method were compared with the experimental values determined for equilenin by Frampton and MacNicol [13]. The root-mean-square deviation (RMSD) values were employed to compare the experimental values with the corresponding theoretical ones. Hence, in **Table 2** are summarized those parameters together with the RMSD values for the three species. The results show very good correlations in the bond lengths and angles (0.008 Å and 0.5º) for equilenin, as expected because its structure is in agreement with the compared one while the RMSD values increase for equilin and estrone to values between 0.054-0.065 Å for bond lengths and to 2.7-1.6 º for bond angles.

Table 2. Calculated geometrical parameters of equilenin, equilin and estrone in gas phase by using the B3LYP/6-31G* method compared with the corresponding experimental values for equilenin taken from Ref [13].

Parameters	**B3LYP/6-31G* Method[a]**			**Experimental[b]**
Bond lengths (Å)	Equilenin	Equilin	Estrone	Equilenin
C20-O2	1.367	1.369	1.369	1.3714(17)
C11=O1	1.211	1.211	1.212	1.220(2)
C17-C19	1.374	1.391	1.389	1.369(2)
C17-C14	1.425	1.402	1.405	1.423(2)
C19-C20	1.416	1.398	1.397	1.411(2)
C20-C18	1.378	1.393	1.393	1.369(2)
C18-C16	1.419	1.399	1.401	1.4243(19)
C16-C15	1.418	1.515	1.519	1.413(2)
C14-C16	1.434	1.405	1.408	1.429(2)
C15-C10	1.373	1.501	1.531	1.369(2)
C5-C10	1.418	1.335	1.532	1.414(2)
C7-C9	1.549	1.543	1.544	1.5433(19)
C7-C4	1.526	1.533	1.532	1.520(2)
C4-C11	1.531	1.531	1.532	1.5118(19)
C4-C3	1.544	1.557	1.549	1.537(2)
C4-C13	1.550	1.550	1.552	1.544(2)
C3-C8	1.543	1.539	1.543	1.535(2)
C8-C12	1.547	1.547	1.547	1.547(2)
C11-C12	1.543	1.543	1.542	1.523(2)
C5-C6	1.392	1.521	1.554	1.381(2)
C5-C3	1.511	1.503	1.529	1.5103(19)
C6-C14	1.434	1.520	1.531	1.4309(19)
C6-C9	1.528	1.561	1.549	1.5234(19)
RMSD	**0.008**	**0.054**	**0.065**	
Bond angles (º)				
C19-C17-C14	121.92	122.04	122.54	121.43(14)
C17-C19-C20	120.14	119.27	119.24	120.34(14)
C18-C20-O2	123.66	117.67	122.88	124.14(14)
C18-C20-C19	119.97	119.52	119.34	120.39(13)
O2-C20-C19	116.36	122.80	117.76	115.46(14)
C20-C18-C16	120.78	121.02	121.36	120.47(14)
C15-C16-C18	121.33	118.32	118.07	121.68(14)
C15-C16-C14	118.80	121.69	122.03	118.77(13)

C7-C9-C6	116.37	113.26	113.33	116.13(13)
C7-C4-C11	117.04	116.71	116.52	116.95(12)
C3-C4-C13	113.61	112.83	114.11	112.60(12)
C5-C3-C8	121.7	123.06	121.58	121.14(13)
C8-C3-C4	104.46	104.36	104.3	103.87(12)
C3-C8-C12	102.41	102.54	102.67	101.83(12)
C8-C12-C11	105.91	105.94	105.85	105.59(13)
C4-C11-O1	126.55	126.48	126.49	125.78(15)
C12-C11-O1	125.53	125.43	125.46	125.78(15)
C4-C11-C12	107.90	108.08	108.04	108.43(13)
RMSD	**0.5**	**2.7**	**1.6**	
Dihedral angles (°)				
C17-C19-C20-O2	-179.87[#]	179.83[#]	-179.93[#]	179.27(14)
O2-C20-C18-C16	179.95	-179.9	179.99	179.87(14)
C14-C6-C9-C7	-177.95	179.12	179.79	-175.62(14)
C9-C7-C4-C11	172.93	169.20	168.68	173.40(14)
C3-C5-C6-C14	177.80	178.02	176.62	175.63(14)
C9-C6-C14-C17	1.38	59.88	33.50	1.3(2)
C5-C6-C9-C7	4.08	51.12	51.99	4.1(2)
C6-C5-C3-C8	157.69	-175.30	-175.53	155.31(15)
C10-C5-C3-C8	-24.82	7.35	-53.49	-28.7(2)
C6-C5-C3-C4	33.05	7.35	59.97	32.65(19)
C7-C4-C3-C5	-61.07	-60.41	-61.28	-61.31(16)
C7-C4-C3-C8	165.20	165.25	165.16	166.61(13)
C5-C3-C8-C12	-168.24	-167.32	-168.01	-167.57(14)
C3-C8-C12-C11	22.20	22.53	21.82	22.97(18)
C13-C4-C11-O1	-88.90	-90.05	-89.14	-91.6(2)
C13-C4-C11-C12	91.11	90.29	90.95	88.83(16)
RMSD	**89.8**	**152.5**	**152.0**	
RMSD[#]	**1.8**	**157.5**	**126.6**	

[a]This work, [b]From Ref [13], [#]Removed value, Letter Bold: RMSD values

Atomic MK and Mulliken charges and Molecular electrosctatic potentials (MEP).

The studies of atomic charges in the three species associated to estrogens are of great interest to explain the structural differences among the B rings where, for instance, equilenin is different from equilin by the unsaturated C5=C10 in B which rotates the C and D rings of the steroid generating the translation of the O1 atom belonging to C11=O1 group, as was experimentally observed for equilin by Sawicki et al [7]. Therefore, the atomic Merz-Kollman (MK) and Mulliken charges on all atoms of three species were calculated in gas phase by using the B3LYP/6-31G* method [44]. Hence, both charges are given in **Table 3** while in **Figure 4** can be seen the behaviours of two charges in the three species. In Fig. 4 are presented the atoms numbering according to Table 3. Both charges on the O1, O2 and C3 atoms that belong to D rings present practically the same behaviours while the higher variations in the charges are observed on the atoms from the C4 to C16 because these atoms are common to the B, C and D rings. Hence, the charges on the C17, C18, C19 and C20 atoms of A rings in the three species basically do not change. Note that the two charges on the C15 atoms are different in equilenin than equilin and estrone because that C atom in equilenin has hybridization sp^2 and one H atom while in the other two species that C15 atoms present sp^3 hybridization containing CH_2 groups. Another important observation is that the two charges on the C11, C12 and C13 in equilin and estrone have approximately the same values while in equilenin the MK charges present lower values. The charges on all H atoms present practically the same positive values in the three species with exception of those atoms linked to O2 atoms where are observed the higher values.

The molecular electrostatic potentials (MEP) values are very interesting parameters to describe the distributions of charges on species containing different rings and OH and C=O groups as, equilin, equilin and estrone and, in particular, their mapped surfaces are useful to find the nucleophilic and electrophilic sites where the reactions with potential biological electrophils and nucleophils reactive take place. Here, the MEP values were calculated from the MK charges for the three species but

significant differences in the values were not found and, for this reason, these values are not presented here [44].

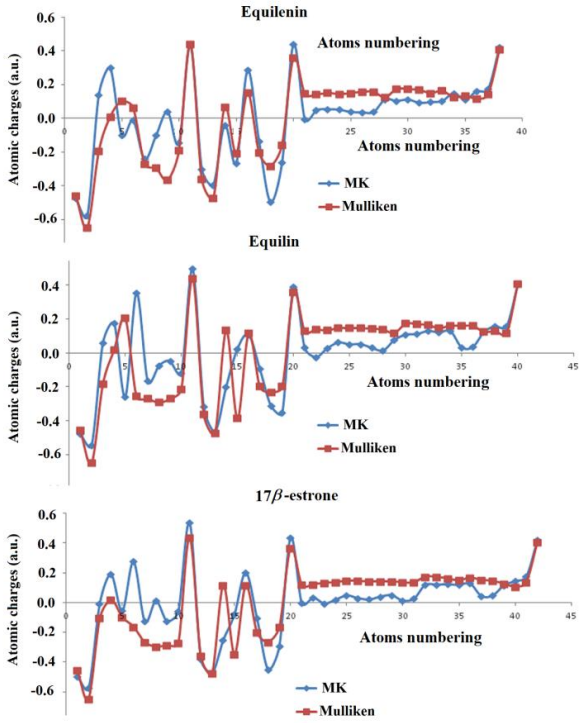

Figure 4. Variations and behaviours of atomic Merz-Kollman (MK) and Mulliken charges on all atoms of equilenin, equilin and estrone steroids in gas phase by using the B3LYP/6-31G* method.

Obviously, the higher negatives values are observed on the O atoms, showing the higher values in the three species the O1 atoms (-22.333—22.331 a.u.) than the O2 ones (-22.284—22.278 a.u.).

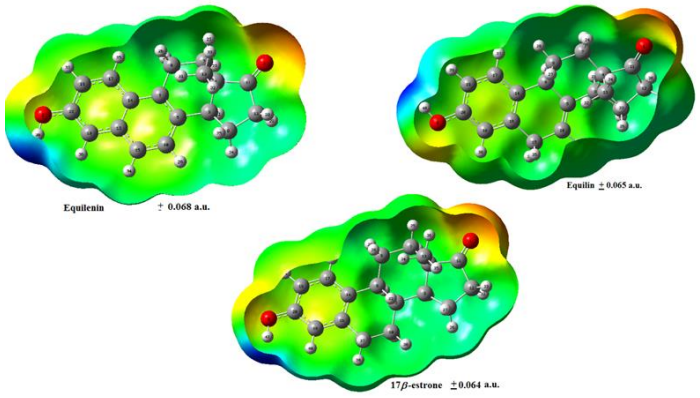

Figure 5. Calculated electrostatic potential surfaces on the molecular surfaces of equilenin, equilin and estrone. Color ranges are indicated in units a.u. B3LYP functional and 6-31G* basis set. Isodensity value of 0.005.

The MEP values on the C atoms have evidenced different values, for instance, from 14.749 to 14.665 a.u. while the H atoms present the less negative values, as expected, showing the lower values on the H atoms linked to the O2 atoms in the three species because these atoms are the most labile. When the mapped surface from **Figure 5** is analyzed the strong red colours are clearly observed on the C=O bonds of the three species indicating that these places are nucleophilic sites while on the OH groups were observed the strong blue colours attributed evidently to electrophilic sites. The green colours in all species are inert sites. Here, a very important observation is the slight orange coloration on the two A and B rings of equilenin, different from the other ones, because both have aromatic naphthalene core, as reported by Frampton and MacNicol for this species [13]. The mapped MEP surfaces in the three species show approximately the same values, as can be seen in Figure 5.

NBO studies.

The analyses of stabilization energies in equilenin, equilin and estrone are important factors taking into account that three of four rings present in their structures are different in the three species showing, in particular the A and B rings of equilenin, aromatic naphthalene core, as reported for this species by Frampton and MacNicol [13]. Hence, in **Table 4** are presented the main delocalization energies for equilenin, equilin and estrone in gas phase by using B3LYP/6-31G* calculations. The careful analysis of results show for the three species four different $\Delta E_{\pi\rightarrow\pi^*}$, $\Delta E_{n\rightarrow\sigma^*}$, $\Delta E_{n\rightarrow\pi^*}$ and $\Delta E_{\pi^*\rightarrow\pi^*}$ interactions where the first and the latter transitions present clearly the higher values in the three species showing the only equilin the higher value in the $\Delta E_{\pi^*\rightarrow\pi^*}$ interaction. In addition, due to the presence of two aromatic rings in equilenin the *π*C14-C16→π*C5-C6* interaction only for this species is observed. On the other hand, the *π*C17-C19→π*C14-C16* interaction is observed only for equilin. Here, a very important resulted is the presence of six $\Delta E_{\pi\rightarrow\pi^*}$ interactions observed only in equilenin due to the presence of two aromatic A and B rings and different from the other ones. Note that in the three species the $\Delta E_{n\rightarrow\sigma^*}$ and $\Delta E_{n\rightarrow\pi^*}$ interactions show low values, as compared with the other ones. When the total energy values are evaluated for the three species it is observed the higher value for equilin, then equilenin and, finally estrone. Hence, equilin is the most stable species, as compared with equilenin and estrone. Probably, the high value evidenced for equilin and its high stability and the lower value observed for estrone could justify the increase in the anti-human estrogenic 17*β*-hydroxysteroid dehydrogenase inhibitory behavior of equilin in relation to estrone, as suggested by Sawicki et al [7].

AIM analyses.

The above NBO studies have revealed the high stability of equilin, as compared with equilenin and estrone showing only this species a high value in the *π*C17-C19→π*C14-C16* transition. Another form different of analyzing the stabilities of these species is through of the Bader's theory of atoms in molecules (AIM) where is possible to examine possible H bonds and/or intra-molecular interactions by using the topological properties with the AIM2000 program [46,47].

Table 3. Atomic MK and Mulliken charges of equilenin, equilin and estrone in gas phase and aqueous solution by using the B3LYP/6-31G* method.

Atoms	B3LYP/6-31G* method[a]					
	MK charges[b]			Mulliken charges[b]		
	Equilenin	Equilin	Estrone	Equilenin	Equilin	Estrone
1 O	-0.473	-0.479	-0.495	-0.458	-0.457	-0.459

2 O	-0.575	-0.547	-0.575	-0.646	-0.647	-0.648
3 C	0.139	0.058	-0.006	-0.195	-0.184	-0.106
4 C	0.298	0.175	0.190	0.009	0.018	0.018
5 C	-0.098	-0.258	-0.056	0.100	0.205	-0.100
6 C	-0.012	0.355	0.276	0.062	-0.256	-0.164
7 C	-0.240	-0.166	-0.125	-0.269	-0.269	-0.268
8 C	-0.101	-0.075	0.010	-0.295	-0.291	-0.297
9 C	0.040	-0.047	-0.126	-0.367	-0.269	-0.289
10 C	-0.145	-0.120	-0.058	-0.191	-0.212	-0.274
11 C	0.434	0.495	0.537	0.439	0.439	0.437
12 C	-0.300	-0.317	-0.381	-0.362	-0.362	-0.361
13 C	-0.395	-0.466	-0.476	-0.473	-0.473	-0.479
14 C	-0.040	-0.200	-0.253	0.068	0.133	0.116
15 C	-0.265	0.025	-0.079	-0.207	-0.385	-0.349
16 C	0.285	0.108	0.202	0.152	0.115	0.114
17 C	-0.136	-0.095	-0.104	-0.205	-0.198	-0.201
18 C	-0.496	-0.314	-0.451	-0.282	-0.230	-0.266
19 C	-0.263	-0.354	-0.292	-0.157	-0.198	-0.165
20 C	0.439	0.389	0.438	0.358	0.357	0.364
21 H	-0.005	0.031	-0.005	0.145	0.129	0.118
22 H	0.049	-0.024	0.034	0.141	0.139	0.121
23 H	0.055	0.027	-0.006	0.150	0.134	0.132
24 H	0.052	0.062	0.019	0.144	0.148	0.135
25 H	0.039	0.051	0.048	0.149	0.147	0.146
26 H	0.036	0.052	0.030	0.157	0.147	0.144
27 H	0.038	0.030	0.021	0.157	0.144	0.141
28 H	0.113	0.015	0.040	0.124	0.138	0.140
29 H	0.104	0.077	0.050	0.174	0.118	0.142
30 H	0.112	0.108	0.013	0.172	0.174	0.135
31 H	0.093	0.112	0.027	0.168	0.171	0.135
32 H	0.097	0.130	0.119	0.149	0.165	0.173
33 H	0.104	0.122	0.120	0.163	0.147	0.171
34 H	0.149	0.129	0.123	0.124	0.162	0.161
35 H	0.111	0.033	0.119	0.134	0.161	0.148
36 H	0.162	0.036	0.128	0.116	0.160	0.166
37 H	0.174	0.125	0.044	0.142	0.125	0.151
38 H	0.423	0.158	0.047	0.408	0.130	0.145
39 H		0.157	0.115		0.116	0.126
40 H		0.403	0.145		0.406	0.106
41 H			0.175			0.136
42 H			0.418			0.406

[a]This work, [b]Atomic units (a.u.)

This study request the calculations of electron density, $\rho(r)$, the Laplacian values, $\nabla^2\rho(r)$, the eigenvalues $(\lambda 1, \lambda 2, \lambda 3)$ of the Hessian matrix and, the $|\lambda 1|/\lambda 3$ ratio in the bond critical points (BCPs) and ring critical points (RCPs) by using the B3LYP/6-31G* method, according to other species with different rings [32-42]. The results for equilenin, equilin and estrone in gas phase species are presented in Table 5. These studies show the RCPs of four A, B, C and D rings for the three species. When the interaction is ionic or of H bonds $\lambda 1/\lambda 3 < 1$ and $\nabla^2\rho(r) > 0$ (closed-shell interaction). Here, only the $\rho(r)$ and $\nabla^2\rho(r)$, parameters are presented in Table 5 because in estrone only the BCP interaction (H39---H29) is observed. The molecular graphic of estrone in gas phase showing the geometry of all its bond critical points (BCP) and ring critical points (RCPs) by using the B3LYP/6-31G* method is given in Figure 6. The figure shows in blue colours the A, B, C and D RCPs of estrone and in red colour the RCPN new formed as a consequence of H39---H29 interaction, not observed in the other two species. When the densities and Laplacian values are analysed it is possible to observe that in equilenin the A and B rings have the same properties values confirming the aromatic naphthalene core of both rings while the $\rho(r)$ and $\nabla^2\rho(r)$ values for A and B are different in equilin and estrone. On the other hand, the D rings of the three species show the higher values, having estrone the

highest value. Also, for estrone is observed an only H bonds interaction (H39---H29) with low density and Laplacian values because the distances between both involved H atoms is 2.058 Å. In addition, the new RCPN has also low values in its properties. These studies clearly evidence the higher stability of estrone in gas phase due to the new H---H interaction which confers to its structure higher stability.

Frontier orbitals and quantum global descriptors studies.

The frontier orbitals are parameters frequently used in the determination of gap values, as suggested by Parr and Pearson [31], because from their differences can be predict the reactivities and, also, with the gap values it is possible to calculate some descriptors of great interest to predict the behaviours of species in different media [32-41]. Hence, the frontier molecular HOMO and LUMO orbitals, gap values and the chemical potential (μ), electronegativity (χ), global hardness (η), global softness (S), global electrophilicity index (ω) and global nucleophilicity index (E) descriptors of equilenin, equilin and estrone in gas phase by using the B3LYP/6-31G* method are summarized in **Table 6**. If the gap values are analyzed it is possible to observe the lower value in equilenin and the higher values for equilin and estrone, where equilin clearly has the highest value and, for this reason, it is the less reactive species in agreement with the higher stability observed by NBO studies. Evidently, the presence of the unsaturated C5=C10 in the B ring of equilin, which rotates the C and D rings of this steroid generating the translation of the O1 atom belonging to C11=O1 group, as was experimentally by Sawicki et al [7], produces a decreasing in its reactivity. On the other hand, equilenin is the most reactive species due to its low gap value. If now the descriptors are analyzed, equilenin has a higher global electrophilicity value while the higher global nucleophilicty values are observed for equilin and estrone. Apparently, the higher global electrophilicity value evidenced by equilenin is related to its higher reactivity and with the less negative nucleophilicity value. The comparisons of these gap values of three steroids species with other such as the free base, cationic and hydrochloride species of alkaloids or antihistaminic agents [48-57] are interesting to know how the different groups and rings present in their structures have influence on their reactivities and behaviours in the different media. Thus, the gap value of 4.5008 eV for equilenin is similar to those observed for the hydrochloride species of morphine (4.5840 eV) and of the R(+) form of promethazine (4.4926 eV) while the values of 5.4695 and 5.4342 eV observed for equilin and estrone, respectively are similar to value predicted for the cationic species of cocaine (5.4468 eV). All these compared species have different fused rings and, also, other groups.

Table 4. Main delocalization energies (in kJ/mol) for equilenin, equilin and estrone in gas phase by using B3LYP/6-31G* calculations.

Delocalization	Equilenin	Equilin	Estrone
$\pi C5\text{-}C6 \rightarrow \pi^*C10\text{-}C15$	76.91		
$\pi C5\text{-}C6 \rightarrow \pi^*C14\text{-}C16$	65.29		
$\pi C10\text{-}C15 \rightarrow \pi^*C5\text{-}C6$	70.18		
$\pi C10\text{-}C15 \rightarrow \pi^*C14\text{-}C16$	68.84		
$\pi C14\text{-}C16 \rightarrow \pi^*C5\text{-}C6$	72.86		
$\pi C14\text{-}C16 \rightarrow \pi^*C10\text{-}C15$	65.92		
$\pi C14\text{-}C16 \rightarrow \pi^*C17\text{-}C19$	76.29	100.61	95.47
$\pi C14\text{-}C16 \rightarrow \pi^*C18\text{-}C20$	64.87	77.04	74.70
$\pi C17\text{-}C19 \rightarrow \pi^*C14\text{-}C16$	57.98	66.42	69.14
$\pi C17\text{-}C19 \rightarrow \pi^*C18\text{-}C20$	79.13	91.63	93.59
$\pi C18\text{-}C20 \rightarrow \pi^*C14\text{-}C16$	74.78	93.88	91.88
$\pi C18\text{-}C20 \rightarrow \pi^*C17\text{-}C19$	62.07	74.57	68.68
$\Delta E_{\pi \rightarrow \pi^*}$	835.12	504.15	493.45
$LP(2)O1 \rightarrow \sigma^*C4\text{-}C11$	90.33	90.41	90.29
$LP(2)O1 \rightarrow \sigma^*C11\text{-}C12$	98.36	97.94	98.06
$\Delta E_{n \rightarrow \sigma^*}$	188.69	188.35	188.35
$LP(2)O2 \rightarrow \pi^*C18\text{-}C20$	124.56	115.12	119.92
$\Delta E_{n \rightarrow \pi^*}$	124.56	115.12	119.92
$\pi^*C14\text{-}C16 \rightarrow \pi^*C5\text{-}C6$	936.28		
$\pi^*C17\text{-}C19 \rightarrow \pi^*C14\text{-}C16$		759.92	
$\pi^*C18\text{-}C20 \rightarrow \pi^*C14\text{-}C16$		848.21	837.84
$\Delta E_{\pi^* \rightarrow \pi^*}$	936.28	1608.13	837.84
ΔE_{Total}	2084.65	2415.75	1639.56

Table 5. Analysis of the Bond Critical Points (BCPs) and Ring critical point (RCPs) for equilenin, equilin and estrone in gas phase by using the B3LYP/6-31G* method.

Parameter[#]	B3LYP/6-31G* Method[a]			
	Equilenin			
	A	B	C	D
ρ(r)	0.0193	0.0192	0.0179	0.0367
$\nabla^2\rho(r)$	0.1512	0.1500	0.1176	0.2482
Equilin				
ρ(r)	0.0199	0.0169	0.0177	0.0365
$\nabla^2\rho(r)$	0.1581	0.1201	0.1117	0.2466
Estrone				
ρ(r)	0.0198	0.0172	0.0176	0.0371
$\nabla^2\rho(r)$	0.1565	0.1152	0.1093	0.2509
	H39-H29	RCPN		
ρ(r)	0.0116	0.0109		
$\nabla^2\rho(r)$	0.0477	0.0550		
Distance, Å	2.058			

[a]This work, [#]In a.u. units

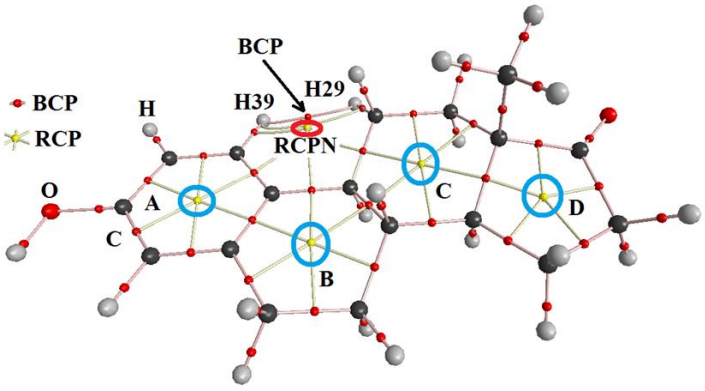

Figure 6. Molecular graphic of estrone in gas phase showing the geometry of all its bond critical points (BCP) and ring critical points (RCPs) by using the B3LYP/6-31G* method. In blue colours are presented the RCPs of A, B, C and D rings and in red colour the only RCPN new while the arrow show the BCP.

Vibrational study.

The structures of equilenin, equilin and estrone species by using B3LYP/6-31G* calculations were optimized with C_1 symmetries. For equilenin are expected 108 vibration modes, for equilin 114 and for estrone 120. All vibration modes present activity in both IR and Raman spectra. In Figures 7 and 8 are compared the experimental available IR and Raman spectra of equilenin in the solid phase taken from Ref [58] with the corresponding predicted by calculations in the gas phase. In Figures 9 and 10 are compared the experimental available IR and Raman spectra of equilin taken from Ref [58] with the corresponding predicted in gas phase by using the hybrid B3LYP/6-31G* method. In Figure 11 can be seen the predicted IR spectrum of estrone in gas phase by using the hybrid B3LYP/6-31G* method while in Figure 12 are compared the experimental available Raman spectrum taken from Ref [17] with the corresponding predicted in gas phase by using the hybrid B3LYP/6-31G* method. All predicted Raman spectra were corrected to intensities by using known equations [42,43].

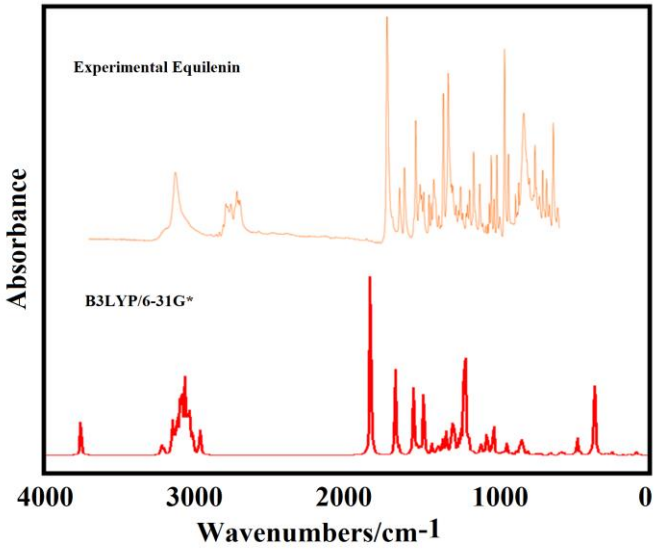

Figure 7. Experimental available IR spectrum of equilenin in solid phase [58] compared with the predicted in gas phase by using the hybrid B3LYP/6-31G* method.

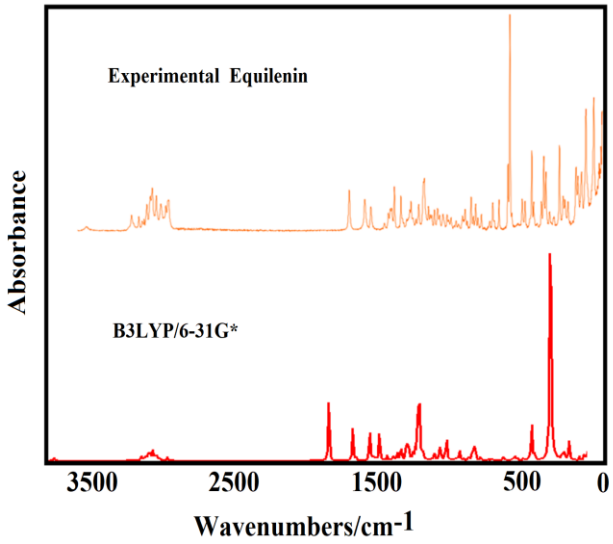

Figure 8. Experimental available Raman spectrum of equilenin in solid phase [58] compared with the predicted in gas phase by using the hybrid B3LYP/6-31G* method.

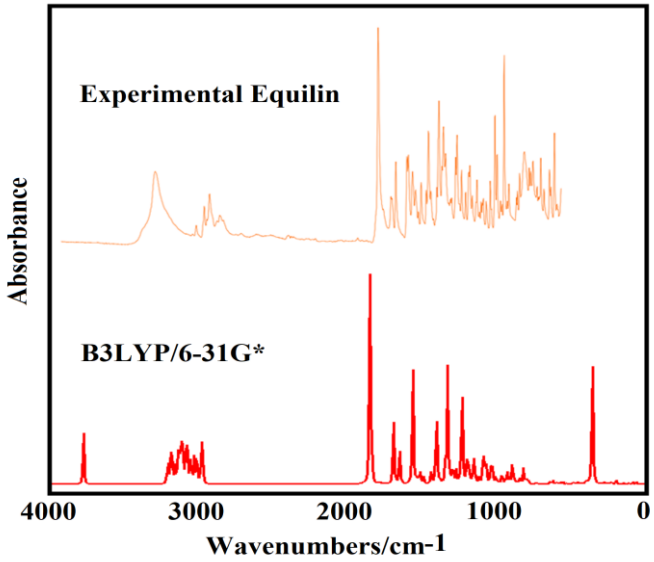

Figure 9. Experimental available IR spectrum of equilin in solid phase [58] compared with the predicted in gas phase by using the hybrid B3LYP/6-31G* method.

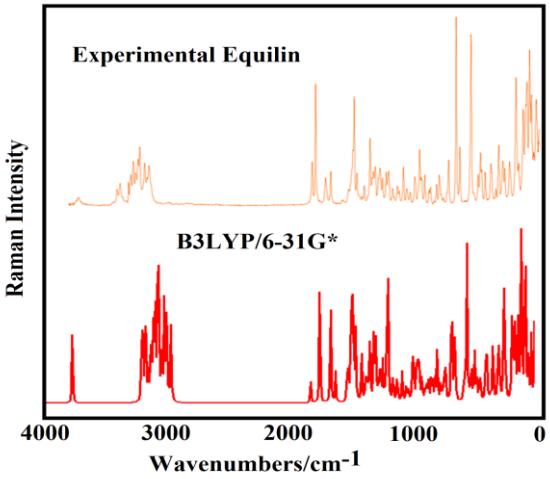

Figure 10. Experimental available Raman spectrum of equilin in solid phase [58] compared with the predicted in gas phase by using the hybrid B3LYP/6-31G* method.

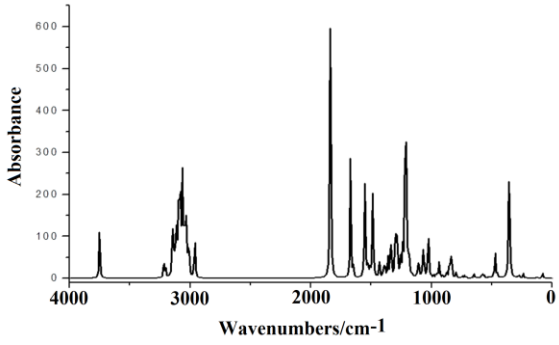

Figure 11. Predicted IR spectrum of estrone in gas phase by using the hybrid B3LYP/6-31G* method.

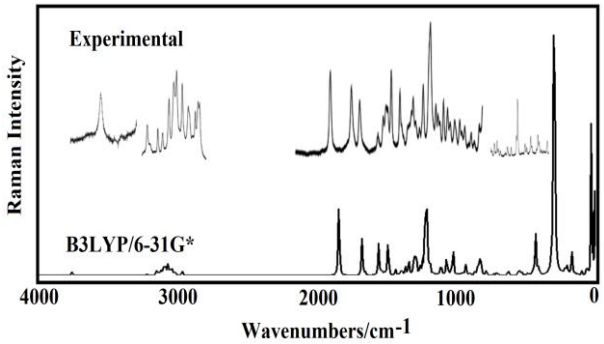

Figure 12. Experimental available Raman spectrum of estrone in solid phase [14] compared with the predicted in gas phase by using the hybrid B3LYP/6-31G* method.

Table 6. Frontier molecular HOMO and LUMO orbitals, gap values and descriptors (in eV) of equilenin, equilin and estrone in gas phase by using the B3LYP/6-31G* method.

B3LYP/6-31G* method[a]			
Orbitals	Equilenin	Equilin	Estrone
HOMO	-5.5321	-5.7933	-5.7607
LUMO	-1.0313	-0.3238	-0.3265
|GAP|	4.5008	5.4695	5.4342
Descriptors			
χ	-2.2504	-2.7348	-2.7171
μ	-3.2817	-3.0586	-3.0436
η	2.2504	2.7348	2.7171
S	0.2222	0.1828	0.1840
ω	2.3928	1.7103	1.7047
E	**-7.3851**	**-8.3644**	**-8.2698**

[a]This work

$\chi = -[E(LUMO) - E(HOMO)]/2$; $\mu = [E(LUMO) + E(HOMO)]/2$; $\eta = [E(LUMO) - E(HOMO)]/2$; $S = \frac{1}{2}\eta$; $\omega = \mu^2/2\eta$; $E = \mu * \eta$

The complete vibrational assignments for the three species were performed with the SQMFF methodology computing their harmonic force fields in gas phase [23]. Hence, the normal internal coordinated were employed and transferable scale factors together with the Molvib program [24,25]. Here, only potential energy contributions ≥ 10% were considered. In **Table 7** are summarized the observed and calculated wavenumbers and assignments for equilenin, equilin and estrone. For equilenin and equilin, the observed bands correspond to the experimental available IR spectra [58] while for estrone corresponds to experimental available Raman spectrum [17]. Then, some assignments for the more important groups are discussed at continuation.

Band Assignments.

4000-2000 cm^{-1} region. In this region are expected the antisymmetric and symmetric stretching modes of CH_3 and CH_2 groups, the aromatic and aliphatic C-H and OH stretching modes. In the three species, the OH stretching modes are predicted at higher wavenumbers than the other ones and, for these reasons, these modes are associated with the IR and Raman bands between 3370 and 3307 cm^{-1}. The groups of IR and Raman bands between 3064 and 3013 cm^{-1} are associated with the aromatic C-H stretching modes while those bands between 2890 and 2822 cm^{-1} are attributed to aliphatic C-H stretching modes. The antisymmetric CH_3 stretching modes are predicted by calculations at higher wavenumbers than the corresponding symmetric modes and, hence, these modes are assigned to the IR and Raman bands 3027 and 2977 cm^{-1}. On the contrary, the corresponding symmetric modes are assigned to the IR bands at 2920 and 2909 cm^{-1}. The antisymmetric and symmetric CH_2 stretching modes are assigned between 2996 and 2858 cm^{-1}, as predicted by the SQM/B3LYP/6-31G* calculations.

2000-1000 cm^{-1} region. Here, the expected modes common to the three species are, C=O, C=C, C-O and C-C stretching modes, deformation, wagging, rocking modes of CH_2 groups, OH deformation, deformation and rocking modes of CH_3 groups and C-H rocking modes. A careful detail of the assignments of those modes for the three species can be seen in Table 7 where the most intense bands are assigned to the C=O and C=C stretching modes. Hence, the intense IR and Raman bands between 1751 and 1496 cm^{-1} can be easily assigned to the C=O and C=C stretching modes corresponding to the three species, as reported for species containing these groups [34-41]. Obviously, those C=O and C=C bonds present double bond characters and, for these reasons, their vibration modes are observed at higher wavenumbers but, the C-C bonds with partial double bond characters are predicted at lower wavenumbers, thus, they can be assigned between 1454 and 1325 cm^{-1}, as observed in Table 7. A very important observation is the differences in the positions of C5-C10 stretching modes because these bonds have different characteristics in the three species. Thus, in equilenin and equilin those bonds present double bond characters (1704-1523 cm^{-1}) and, as a consequence they are observed at higher wavenumbers than the corresponding to estrone while, in estrone, that mode is predicted to 1085 cm^{-1}. The other C-C stretching modes expected in the three species with simple bond characters can be assigned from 1001 up to 553 cm^{-1}. Here, it is notable the difference in the C4-CH_3 stretching modes (C4-C13) because in the three species these modes are predicted coupled with other vibration modes and in different positions. In the three species the C20-O2 stretching modes are predicted in approximately the same regions, hence, they can be assigned to the intense and of media intensities IR and Raman bands between 1293 and 1281 cm^{-1}. In the same way, the OH deformation modes for the three species are predicted in the same regions, therefore, the bands observed between 1171 and 1137 cm^{-1} are assigned to these vibration modes.

Table 7. Observed and calculated wavenumbers (cm^{-1}) and assignments of equilenin, equilin and estrone in gas phase by using the B3LYP/6-31G* method.

Experimental			B3LYP/6-31G* Method[a]					
			Equilenin		Equilin		Estrone	
Equilenin	**Equilin**	**Estrone**						
IR[c]	IR[d]	Raman[e]	SQM[b]	Assignments[a]	SQM[b]	Assignments[a]	SQM[b]	Assignments[a]
3331m	3307m	3370w	3592	νO2 -H38	3597	νO2-H40	3594	νO2-H42
		3093sh	3092	νC17-H35	3062	νC18-H38	3086	νC19-H41
		3075w	3075	νC19-H37	3054	νC17-H37	3070	νC17-H39
3064w	3040w	3062sh	3066	νC10-H28	3034	νC19-H39	3017	νC18-H40
		3027w	3046	νC15-H34	3033	νC10-H29	3010	$\nu_a CH_3$
3025w	3013w	3005w	3030	νC18-H36	3012	$\nu_a CH_3$	2995	$\nu_a CH_3$

			3009	ν_aCH_3	2994	ν_aCH_3	2985	ν_aCH_2(C8)
2996w		2977m	2993	ν_aCH_3	2987	ν_aCH_2(C8)	2974	ν_aCH_2(C12)
		2953m	2986	ν_aCH_2(C8)	2975	ν_aCH_2(C12)	2966	ν_aCH_2(C9)
			2975	ν_aCH_2(C12)	2970	ν_aCH_2(C9)	2959	ν_aCH_2(C7)
2964sh	2957w	2946m	2968	ν_aCH_2(C7)	2960	ν_aCH_2(C7)	2951	ν_aCH_2(C10)
2945m			2942	ν_sCH_2(C8)	2945	ν_sCH_2(C8)	2940	ν_sCH_2(C8)
2937sh			2937	ν_aCH_2(C9)	2936	ν_sCH_2(C12)	2936	ν_sCH_2(C12)
	2920m		2936	ν_sCH_2(C12)	2934	ν_sCH_3	2935	ν_aCH_2(C15)
2909m			2932	ν_sCH_3	2931	ν_sCH_2(C9)	2933	ν_sCH_3
2873sh		2918m	2921	ν_sCH_2(C7)			2923	ν_sCH_2(C9)
					2912	ν_sCH_2(C7)	2913	ν_sCH_2(C7)
2861m			2901	ν_sCH_2(C9)			2905	ν_sCH_2(C10)
		2890w			2891	ν_aCH_2(C15)	2888	νC5-H22
	2866w	2858w			2873	ν_sCH_2(C15)	2887	ν_sCH_2(C15)
	2846w	2845w			2840	νC6-H22	2840	νC3-H21
2834m	2822w		2831	νC3-H21	2828	νC3-H21	2833	νC6-H23
1711vs	1714vs	1751s	1771	νC11=O1	1769	νC11=O1	1769	νC11=O1
1615m	1622m		1629	νC17-C19	1704	νC5-C10		
1615m	1591s	1652s	1604	νC10-C15	1625	νC18-C20,νC17-C19 νC14-C17	1616	νC17-C19,νC16-C18
1580m	1511s	1589m	1572	νC5-C6	1586	νC19-C20,νC16-C14	1592	νC19-C20,νC18-C20
1496s			1523	νC19-C20,νC5-C10				
1496s	1501s	1504w	1484	βC10-H28	1503	βC17-H37,βC18-H38	1504	βC17-H39,νC16-C14
	1470s	1478w	1477	δCH_2(C8)	1476	δ_aCH_3	1477	δCH_2(C8),δ_aCH_3
1469w	1470s		1470	δ_aCH_3	1472	δCH_2(C8)	1472	δ_aCH_3
1469w			1465	δCH_2(C7)			1461	δCH_2(C8),δ_aCH_3
		1454w			1459	δCH_2(C7),δCH_2(C8)	1458	δCH_2(C9)
1459m	1450w	1447s	1454	δ_aCH_3	1454	νC16-C18	1458	δCH_2(C10)
	1450w				1450	$\delta_aCH_3\delta CH_2$(C9)	1445	δCH_2(C7)
1451mw			1445	δCH_2(C9)	1445	δCH_2(C7)	1443	δCH_2(C15)
1434m	1423w		1420	βC18-H36,νC17-C19	1435	δCH_2(C15)	1439	δCH_2(C15),βC19-H41
	1406m		1414	δCH_2(C12)	1416	δCH_2(C12)	1417	δCH_2(C12)
1394m		1400m	1384	νC18-C20	1395	ρ'C3-H21	1404	ρ' C3-H21,ρC5-H22
1374w			1378	wagCH_2(C9)			1385	wagCH_2(C10)
	1368sh		1372	δ_sCH_3	1373	δ_sCH_3 wagCH_2(C9)	1370	δ_sCH_3
		1364sh	1365	δ_sCH_3	1366	δ_sCH_3	1367	wagCH_2(C9)
	1356s	1354w			1360	wagCH_2(C15)	1361	wagCH_2(C15)
1358m			1355	νC16-C14			1356	wagCH_2(C7)
1348sh	1342sh	1347w	1351	wagCH_2(C7) ρ'C3-H21	1352	wagCH_2(C7)	1349	ρC6-H23,ρ'C5-H22,ρCH_2(C9)
		1333w			1337	wagCH_2(C9),ρC6-H22	1337	ρC3-H21
	1322vw		1325	νC6-C14	1326	βC10-H29	1316	ρCH_2(C10)
1318w		1314w	1315	ρC3-H21	1309	ρC3-H21	1312	wagCH_2(C8)
			1301	wagCH_2(C8)	1302	wagCH_2(C8)	1308	ρ'C6-H23
	1295sh	1293m			1297	ρ'C6-H22	1297	νC20-O2
1284s	1281s	1293m	1285	νC16-C18,νC20-O2	1287	wagCH_2(C12),ρ'C6-H22	1290	ρCH_2(C15)
	1281s				1279	νC20-O2	1279	wagCH_2(C12)
1256sh		1259s	1272	wagCH_2(C12)	1270	wagCH_2(C12)	1263	ρCH_2(C7)
1247s			1259	νC14-C17			1256	βC18-H40
	1259sh	1249s	1247	ρCH_2(C7),βC18-H36	1250	ρCH_2(C7)	1248	νC4-C11
	1250s	1236w	1246	νC4-C11	1246	βC18-H38	1246	ρCH_2(C10)
1223sh	1233m	1227w	1230	ρCH_2(C9),νC3-C5	1231	νC4-C11	1223	ρCH_2(C15)
1213m		1215w	1210	ρCH_2(C9),νC5-C10	1209	ρCH_2(C8)	1207	ρCH_2(C8), ρCH_2(C12)

1207sh	1199w	1197w	1205	ρCH_2(C8)	1203	ρCH_2(C15)	1203	ρCH_2(C15), νC6-C14
	1191w	1193w			1189	νC6-C14		
1185w			1178	βC15-H34	1184	ρCH_2(C9),ρCH_2(C12)	1183	νC6-C14,νC16-C18
1167w	1161s	1171w	1175	βC18-H36,νC15-C16	1167	δO2-H40	1162	βC19-H41
							1156	δO2-H42
1153m	1151s		1148	ρCH_2(C12)	1152	βC19-H39	1153	δO2-H42,ρCH_2(C10)
		1144w	1146	βC19-H37	1149	νC3-C5	1149	δO2-H42
1137sh	1137sh	1140w	1145	δO2-H38	1142	νC3-C5,βC18-H38	1127	ρCH_2(C12),ρCH_2(C7)
1107sh	1119m	1120w	1126	ρCH_2(C7)	1121	ρCH_2(C7)	1121	ρCH_3
	1092w	1101w			1108	βR_1(A1),νC15-C16	1090	νC3-C5,νC3-C8
1084m		1086w	1084	νC3-C8,νC6-C9			1085	νC5-C10
1054s	1067m	1056w	1054	ρCH_3	1069	νC3-C8	1057	νC5-C6
1040sh	1060m	1044w	1046	νC11-C12,νC7-C9	1037	ρCH_3	1038	νC6-C9
	1044w	1021w			1032	νC6-C9,νC5-C6	1029	νC11-C12
1008m	1012m	1011w	1010	ρCH_2(C8),νC4-C13	1021	νC10-C15	1016	νC10-C15
982w	994w	990w	996	ρ'CH_3	990	νC7-C9	994	βR_1(A1)
	980w				985	ρ'CH_3	987	νC4-C13
960w			969	νC7-C9			973	ρ'CH_3
		965w	954	γC17-H35			963	νC7-C9
	962w		950	γC10-H28,γC15-H34	959	νC7-C9,νC8-C12		
	944w	952w	950	νC8-C12	950	νC8-C12	947	νC8-C12
932m	938sh	938w	946	γC10-H28,γC15-H34	933	νC8-C12,νC4-C13	941	γC17-H39
	930sh				930	γC10-H29,$\tau_w$$CH_2$(C15)		
918s			924	νC7-C9	921	γC17-H37		
	915m	923w			918	νC10-C15	915	νC10-C15,νC20-O2
896m	904sh	902w	908	$\tau_w$$CH_2$(C7) $\tau_w$$CH_2$(C9)	890	βR_1(A2)	901	$\tau_w$$CH_2$(C8)
873s	881s		888	νC4-C13	876	γC18-H38	883	$\tau_w$$CH_2$(C10),$\tau_w$$CH_2$(C9)
855w	865s	860sh	851	ρCH_3	871	γC18-H38	867	νC4-C13
849sh		849w	843	γC18-H36			840	γC18-H40
	841w	830w	824	γC19-H37	830	$\tau_w$$CH_2$(C7)	826	γC19-H41
817vs	827w	823sh	811	βR_1(A2)	816	$\tau_w$$CH_2$(C15),γC10-H29	818	γC19-H41,γC18-H40
817vs	815vs		804	γC18-H36,γC15-H34	800	$\tau_w$$CH_2$(C7)	805	$\tau_w$$CH_2$(C15)
785s	763w	791w	792	γC15-H34	796	γC19-H39	790	$\tau_w$$CH_2$(C12),νC4-C13
779sh	781w		780	$\tau_w$$CH_2$(C8) $\tau_w$$CH_2$(C12) νC11=O1	781	$\tau_w$$CH_2$(C8)		
	775sh				770	βR_1(A2)	777	$\tau_w$$CH_2$(C9),νC3-C4
731w	727sh	736m	755	τR_1(A2)	753	τR_1(A1) $\tau_w$$CH_2$(C7)	763	$\tau_w$$CH_2$(C7)
717w		722s	723	βR_1(A1)			727	βR_3(A1),βR_1(A1),νC15-C16
708m	720w		711	τR_1(A1)	717	βR_3(A1)	704	τR_1(A1)
	706m				691	τR_1(A1)		
670s	672m	676w	684	νC4-C13,$\tau_w$$CH_2$(C9)	670	$\tau_w$$CH_2$(C9) νC4-C13	680	τR_1(A1),νC4-C13
646sh		646w	647	τR_1(A1) τR_2(A1)			633	βR_1(A4),βR_1(A2)
628w	626m	629w	617	βR_1(A3)	625	βR_2(A2)	621	γC20-O2,τR_1(A1)
582s	608m		592	βR_2(A4),νC4-C7	597	νC11-C12,νC4-C7		
574sh	582w	581w	585	γC20-O2	584	βR_2(A4)	583	βR_2(A4),νC4-C7
	552m	577sh			569	γC20-O2	562	νC11-C12 βC11=O1
550w	532m	556vw	553	βR_2(A2),νC11-C12 βC11=O1	546	βR_1(A3)	561	γC20-O2
		529w	537	$\tau_w$$CH_2$(C12)	537	$\tau_w$$CH_2$(C12),γC11=O1	537	$\tau_w$$CH_2$(C12),γC11=O1
527m	527sh		530	τR_3(A2)	533	βC11=O1		
515sh		513m	513	βR_2(A1) βR_1(A4)			512	βR_2(A1)
	515sh	500w	502	τR_2(A2) ButtC16-C14	511	βR_2(A1) βR_1(A4)	505	βR_2(A2)
		476w			474	βR_3(A2)	474	βR_3(A3),βR_1(A3)
495m	493m		490	βR_3(A2),βC20-O2	462	βC20-O2	467	βC20-O2

473w		448w	476	βR_3(A1)			443	βR_3(A2)
	455s	448w			432	τR_2(A1)	435	τR_2(A1),ButtC16-C14
443s	439w		425	βR_2(A3) βR_3(A3)	424	βR_2(A3),βR_3(A3)		
411w		416w	409	τR_2(A1)			403	βR_2(A3)
			379	ρ'C4-C13			379	ρ'C4-C13
			352	βC20-O2	383	ρ'C4-C13,ρC4-C13		
			350	τO2-H42	368	τR_2(A1),τR_1(A1)	363	τR_2(A1)
			336	τO2-H42	335	τR_2(A2),βC20-O2	341	βC20-O2,τR_1(A3)
					315	τO2-H40	318	τO2-H42
			284	ρC4-C13	291	τR_1(A3)	296	τR_1(A3)
			281	ρ'C4-C13	279	ρ'C4-C13,ρC4-C13	280	ρC4-C13
			248	τR_3(A1),ButtC5-C6	265	τR_1(A2)	264	βR_2(A2)
			243	δC7C4C11	241	τR_2(A2),δC7C4C11	237	νC6-C14
			229	τR_1(A3)	221	τR_2(A4),τR_2(A3)	234	ButtC5-C6,τR_3(A1)
			196	τR_2(A4)	218	τR_2(A2)	223	τR_2(A2),τR_1(A2)
			189	$\tau_w CH_3$	193	τR_2(A4),δC7C4C11	200	$\tau_w CH_3$
					182	ButtC16-C14	185	δC7C4C11,τR_2(A4)
			164	$\tau_w CH_3$,δC7C4C11	156	$\tau_w CH_3$	160	$\tau_w CH_3$
			129	δC7C4C11				
			121	τR_3(A1)	141	τR_3(A1)	128	τR_2(A3)
			95	τR_1(A4)	105	τR_1(A4)	114	τR_2(A2),τR_1(A4)
			60	τR_3(A3)	78	τR_2(A3),τR_3(A3)	79	τR_1(A4),τR_3(A1)
			43	τR_2(A3) ButtC5-C6	55	ButtC5-C6	56	ButtC5-C6
					37	τR_3(A2)	32	τR_3(A2),τR_3(A3)

Abbreviations: ν, stretching; β, deformation in the plane; γ, deformation out of plane; wag, wagging; τ, torsion; β_R, deformation ring; τ_R, torsion ring; ρ, rocking; τw, twisting; δ, deformation; a, antisymmetric; s, symmetric; (A_1), Ring A; (A_2), Ring B; (A_3), Ring C; (A_4), Ring D. [a]This work, [b]From scaled quantum mechanics force field, [c]From Ref [58], [d]From Ref [58], [e]From Ref [17].

1000-10 cm^{-1} region. The main vibration modes expected in this region are, for instance, some C-C stretching modes already analyzed in the previous section, the C-H out-of-plane deformation, CH_2 and CH_3 twisting modes, deformations and torsions of A, B, C and D rings and torsions OH groups. The OH torsions are predicted in the same regions for the three species (350-315 cm^{-1}) but they were not assigned because there are not bands experimentally observed in that region. In the same way, the CH_3 twisting modes were predicted by SQM calculations between 200 and 156 cm^{-1} but not assigned for the same reason explained for the OH torsion modes. Here, the C7C4C11 deformation mode in equilenin is predicted between 164 and 129 cm^{-1} different from equilin and estrone where are observed between 193 and 185 cm^{-1}. This important difference can clearly be attributed to unsaturated C=C in B of equilin which rotates the C and D rings of the steroid generating the translation of the O1 atom belonging to C11=O1 group, as was experimentally observed for this species by Sawicki et al [7]. The deformations and torsions of A, B, C and D rings and torsions modes are assigned according to calculations, as observed in Table 7.

Force Fields.

The harmonic force constants are important parameters that explain the force of different bonds and, in particular, in equilenin, equilin and estrone are useful due to the clear difference in their structures. Hence, the main scaled force constants were calculated for the three species from their corresponding harmonic force fields by using the 6-31G* method, the SQMFF methodology [23,24] and the Molvib program [25]. Thus, in **Table 8** are compared these parameters for the three species in gas phase by using that level of theory.

Table 8. Scaled internal force constants for equilenin, equilin and estrone in gas phase by using the B3LYP/6-31G* method[a].

Force	Equilenin	Equilin	Estrone
f(νC=O)	12.43	12.42	12.41
f(νO-H)	7.22	7.24	7.23
f(νC-O)	5.98	5.94	5.94
f(νCH$_2$)	4.80	4.76	4.76
f(νC-H)$_{A,B}$	5.15	4.08	5.13
f(νC=C)	6.35	6.86	6.48
f(νC-CH$_3$)	3.67	3.67	3.61
f(δCH$_2$)	0.74	0.73	0.73
f(δOH)	0.74	0.74	0.74

Units are mdyn Å^{-1} for stretching and mdyn Å rad^{-2} for angle deformations, [a]This work

Analysing the results it is observed that some values remain practically constants in the three species, indicating clearly that the involved groups do not present changes in their structures. Hence, the *f(νC=O), f(νO-H), f(νC-O), f(νCH$_2$), f(νC-CH$_3$), f(δCH$_2$)* and *f(δOH)* force constants in the three species have the

same values. On the contrary, the $f(\nu C\text{-}H)_{A,B}$ and $f(\nu C{=}C)$ force constants are different in the three species because in equilenin the A and B rings are aromatic and, for these reasons, this species has higher number of CH aromatics while in equilin the presence of other CH_2 group, instead of C-H, in the B ring decrease the number of C-H with aromatic characteristics. Hence, the $f(\nu C\text{-}H)_{A,B}$ force constant has lower value in equilin. Moreover, in equilin the presence of a C=C in the B ring increase the number of C=C increasing the corresponding force constant to 6.86 mdyn $Å^{-1}$. The force constants predicted for the three species present value similar to the observed in other species containing similar groups [32,34-41,48-54].

4. CONCLUSIONS

Here, three species associated with estrogens were studied, equilenin, equilin and estrone. Their molecular structures were theoretically studied in gas phase with the hybrid B3LYP/6-31G* method. NBO, AIM and frontier orbital calculations were computed to study the structural, electronic, topological and vibrational properties of those three species at the same level of theory. Estrone presents higher dipole moment and volume values, as compared with equilin and equilenin, however, equilin presents higher volume than equilenin but lower dipole moment value. The unsaturated C=C in B ring of equilin, which rotates the C and D rings of the steroid generating the translation of the O1 atom belonging to C11=O1, could probably explain those differences. Differences in the dihedral angles in the three species clearly explain the structural differences in their properties. The analyses of MK and Mulliken charges evidence the higher variations on the C atoms common to the B, C and D rings in the three species. The mapped MEP surfaces show that both A and B rings of equilenin are different from the other ones corresponding to the other two species because they have aromatic naphthalene core, as was evidenced experimentally. The NBO studies support the higher stability of equilin, in relation to equilenin and estrone while the AIM analyses reveal the higher stability for estrone. The gap values suggest that equilenin is the most reactive species due to its higher global electrophilicity value, in agreement with the higher stability observed for this species while the higher global nucleophilicty values are observed for equilin and estrone. Here, the harmonic force fields, scaled force constants and the complete assignments of 108, 114 and 120 vibration modes for equilenin, equilin and estrone, respectively are reported for first time.

5. REFERENCES

1. Norton, D.A.; Kartha, G.; Lu, C.T. The Crystal and Molecular Structures of 4-Bromoestrone. *Acta Cryst.* **1963**, *16*, 89-94, http://dx.doi.org/10.1107/S0365110X63000219
2. Hauptman, H.; Fisher, J.; Hancock, H.; Norton, D.A. Phase Determination for the Estriol Structure. *Acta Cryst.* **1969**, *B25*, 811-814, https://doi.org/10.1107/S0567740869003086.
3. Duax, W.L.; Rohrer, D.C.; Blessing, R.H.; Strong, P.D. Steroid Structure and Function. III. Conformational Transmission in 1,3,5(10)-Estratrienes. *Acta Cryst.* **1979**, *B35*, 2656-2664, https://doi.org/10.1107/S0567740879010086.
4. Bieri, J.H.; Prewo, R.; Brianso, J.L.; Piniella, J.F. 10fl-Hydroxy-l,4-estradiene-3,17-dione. *Acta Cryst.* **1985**, *C41*, 1530-1532, https://doi.org/10.1107/S0108270185008435
5. Lábas, A.; Krámos, B.; Oláh, J. Combined Docking and Quantum Chemical Study on CYP-mediated Metabolism of Estrogens in Man. *Acta Cryst.* **1985**, *C41*, 1530-1532, https://doi.org/10.1021/acs.chemrestox.6b00330.
6. Duax, W.L.; Griffin, J.F.; Strong, P.D.; Wood, K.J. 1lβ-Hydroxy-9β-estrone. *Acta Cryst.* **1989**, *C45*, 930-932
7. Sawicki, M.W.; Lib, N.; Ghosh, D. Equilin. *Acta Cryst.* **1999**, *C55*, 425-427, https://doi.org/10.1107/S0108270198013250.
8. Duax, W.L.; Griffin, J.F.; Strong, P.D. Structure of 9fl-Estrone. *Acta Cryst.* **1991**, *C47*, 1096-1097, https://doi.org/10.1107/S0108270190011763.
9. Kirschbaum, K.; Poomani, K.; Parrish, D.A.; Pinkerton, A.A.; Zhurova, E. A standard local coordinate system for multipole refinements of the estrogen core structure. *J. Appl. Cryst.* **2003**, *36*, 1464-1466, https://doi.org/10.1107/S0021889803017825.
10. Minaev, V.A.; Minaev, B.F.; Hovorun, D.M. Vibrational spectra of the steroid hormones, estradiol and estriol, calculated by density functional theory. The role of low-frequency vibrations. *Ukr Biokhim Zh.*, **2008**, *80*, 82-95.
11. Türker, L.; Bayar, Ç.Ç. A DFT Study on Estrone –TNT Interaction. *Z. Anorg. Allg. Chem.* **2013**, *639*, 1871–1875, https://doi.org/10.1002/zaac.201300239.
12. Albuquerque, C.D.L.; Nogueira, R.B.; Poppi, R.J. Determination of 17β-estradiol and noradrenaline in dog serum using surface-enhanced Raman spectroscopy and random Forest, *Microchemical J.* **2016**, *128*, 95–101, https://doi.org/10.1016/j.microc.2016.04.012.
13. Frampton, C.S.; MacNico, D.D. Structure of Equilenin at 100 K: an estrone-related steroid. *Acta Cryst.* **2017**, *E73*, 1223–1226, https://doi.org/10.1107/S2056989017010532.
14. Liu, S.; Cheng, R.; Chen, Y.; Shi, H.; Zhao, G.A simple one-step pretreatment, highly sensitive and selective sensing of 17β-estradiol in environmental water samples using surface-enhanced Raman spectroscopy, *Sensors and Actuators*. **2018**, *B254*, 1157–1164, https://doi.org/10.1021/acsami.5b12866.
15. Lima do Nascimento, M.T.; de Oliveira Santos, A.D.; Felix, L.C.; Gomes, G.; de Oliveira Sá, M.; Lima da Cunha, D.; Vieira, N.; Hauser-Davis, R.A.; Neto, J.A.B.; Bila, D.M. Determination of water quality, toxicity and estrogenic activity in a nearshore marine environment in Rio de Janeiro, Southeastern Brazil. *Ecotoxicology and Environmental Safety* **2018**, *149* 197–202, https://doi.org/10.1016/j.ecoenv.2017.11.045.
16. Korn, V. Effects of Estrone and Temperature on the Predator-Prey Relationship Between Bluegill Sunfish and Fathead Minnows. *Doctoral Thesis, St. Cloud State University* **2018**.
17. Vedad, J.; Mojica, E-R.E.; Desamero, R.Z.B. Raman spectroscopic discrimination of estrogens. *Vibrational Spectroscopy* **2018,** *96*, 93–100, https://doi.org/10.1016/j.vibspec.2018.02.011
18. Funder, J.W.; Krozowski, Z.; Myles, K.; Sato, A.; Sheppard, KE.; Young, M. Mineralocorticoid receptors, salt, and hypertension. *Recent Prog Horm Res.* **1997**, *52*, 247–260.
19. Gupta, B.B.P.; Lalchhandama, K. Molecular mechanisms of glucocorticoid action. *Current Science* **2002**, *83*, 1103–1111.
20. Frye, C.A. Steroids, reproductive endocrine function, and affect. A review. *Minerva Ginecol.* **2009**, *61*, 541–562.

21. Marcinkowska, E.; Wiedłocha, A. Steroid signal transduction activated at the cell membrane: from plants to animals. *Acta Biochim Pol.* **2002**, *49*, 735–745.
22. Wang, C.; Liu, Y.; Cao, J.M. G protein-coupled receptors: Extranuclear mediators for the non-genomic actions of steroids. *International Journal of Molecular Sciences* **2014**, *15*, 15412–25, https://dx.doi.org/10.3390%2Fijms150915412.
23. Pulay, P.; Fogarasi, G.; Pongor, G.; Boggs, J.E.; Vargha, A. Combination of theoretical ab initio and experimental information to obtain reliable harmonic force constants. Scaled quantum mechanical (QM) force fields for glyoxal, acrolein, butadiene, formaldehyde, and ethylene. *J. Am. Chem. Soc*. **1983**, *105*, 7073, https://doi.org/10.1021/ja00362a005.
24. a) Rauhut, G.; Pulay, P. Transferable Scaling Factors for Density Functional Derived Vibrational Force Fields. *J. Phys. Chem*. **1995**, 99: 3093-3100, https://doi.org/10.1021/j100010a019
25. Sundius, T. Scaling of ab-initio force fields by MOLVIB. *Vib. Spectrosc*. **2002**, *29*, 89-95, https://doi.org/10.1016/S0924-2031(01)00189-8.
26. Lee, C.; Yang, W.; Parr, R.G. Development of the Colle-Salvetti correlation-energy formula into a functional of the electron density. *Phys. Rev*., **1988**, *B37*, 785-789, https://doi.org/10.1103/physrevb.37.785.
27. Becke, A.D. Density-functional exchange-energy approximation with correct asymptotic behavior. *Phys. Rev*. **1988**, *A38*, 3098-3100, https://doi.org/10.1103/PhysRevA.38.3098.
28. Nielsen, A.B.; Holder, A.J. Gauss View 3.0. User's Reference, Gaussian Inc., Pittsburgh, PA, **2000–2003**.
29. Frisch, M.J.; Trucks, G.W.; Schlegel, H.B.; Scuseria, G.E.; Robb, M.A.; Cheeseman, J.R.; Scalmani, G.; Barone, V.; Mennucci, B.; Petersson, G.A.; Nakatsuji, H.; Caricato, M.; Li, X.; Hratchian, H.P.; Izmaylov, A.F.; Bloino, J.; Zheng, G.; Sonnenberg, J.L.; Hada, M.; Ehara, M.; Toyota, K.; Fukuda, R.; Hasegawa, J.; Ishida, M.; Nakajima, T.; Honda, Y.; Kitao, O.; Nakai, H.; Vreven, T.; Montgomery, J.A.; Peralta, J.E.; Ogliaro, F.; Bearpark, M.; Heyd, J.J.; Brothers, E.; Kudin, K.N.; Staroverov, V.N.; Kobayashi, R.; Normand, J.; Raghavachari, K.; Rendell, A.; Burant, J.C.; Iyengar, S.S.; Tomasi, J.; Cossi, M.; Rega, N.; Millam, J.M.; Klene, M.; Knox, J.E.; Cross, J.B.; Bakken, V.; Adamo, C.; Jaramillo, J.; Gomperts, R.; Stratmann, R.E.; Yazyev, O.; Austin, A.J.; Cammi, R.; Pomelli, C.; Ochterski, J.W.; Martin, R.L.; Morokuma, K.; Zakrzewski, V.G.; Voth, G.A.; Salvador, P.; Dannenberg, J.J.; Dapprich, S.; Daniels, A.D.; Farkas, O.; Foresman, J.B.; Ortiz, J.; Cioslowski, J.; Fox, D.J. Gaussian, Inc., Wallingford CT, **2009**.
30. Ugliengo, P. Moldraw Program. *University of Torino, Dipartimento Chimica IFM, Torino, Italy*, **1998.**
31. Paar, R.G.; Pearson, R.G. Absolute hardness: companion parameter to absolute electronegativity. *J. Am. Chem*. Soc. **1983**, *105*, 7512-7516, https://doi.org/10.1021/ja00364a005.
32. Romani, D.; Brandán, S.A.; Márquez, M.J.; Márquez, M.B. Structural, topological and vibrational properties of an isothiazole derivatives series with antiviral activities. *J. Mol. Struct.* **2015**, *1100*, 279-289, https://doi.org/10.1016/j.molstruc.2015.07.038.
33. Romani, D.; Tsuchiya, S.; Yotsu-Yamashita, M.; Brandán, S.A. Spectroscopic and structural investigation on intermediates species structurally associated to the tricyclic bisguanidine compound and to the toxic agent, saxitoxin. *J. Mol. Struct*., **2016**, *1119*, 25-38, http://dx.doi.org/10.1016/j.molstruc.2016.04.039.
34. Romano, E.; Castillo, M.V.; Pergomet, J.L.; Zinczuk, J.; Brandán, S.A. Synthesis, structural and vibrational analysis of (5,7-Dichloro-quinolin-8-yloxy) acetic acid. *J. Mol. Struct.* **2012**, *1018*, 149–155, https://doi.org/10.1016/j.molstruc.2012.03.013.
35. Iramain, M.A.; Davies, L.; Brandán, S.A. Structural and spectroscopic differences among the Potassium 5-hydroxypentanoyltrifluoroborate salt and the furoyl and isonicotinoyl salts. *J Mol. Struct*. **2019**, *1176*, 718-728, https://doi.org/10.1016/j.molstruc.2019.02.010.
36. Issaoui, N.; Ghalla, H.; Brandán, S.A.; Bardak, F.; Flakus, H.T.; Atac, A.; Oujia, B. Experimental FTIR and FT-Raman and theoretical studies on the molecular structures of monomer and dimer of 3-thiopheneacrylic acid. *J. Mol. Struct***. 2017**, *1135*, 209-221, https://doi.org/10.1016/j.molstruc.2017.01.074.
37. Minteguiaga, M.; Dellacassa, E.; Iramain, M.A.; Catalán, C.A.N.; Brandán, S.A. FT-IR, FT-Raman, UV-Vis, NMR and structural studies of Carquejyl Acetate, a component of the essential oil from *Baccharis trimera* (Less.) DC. (Asteraceae). *J Mol. Struct*. **2019**, *1177*, 499-510, https://doi.org/10.1016/j.molstruc.2018.10.010.
38. Minteguiaga, M.; Dellacassa, E.; Iramain, M.A.; Catalán, C.A.N.; Brandán, S.A. A structural and spectroscopic study on carquejol, a relevant constituent of the medicinal plant Baccharis trimera (Less.) DC. (Asteraceae). *J. Mol. Struct*. **201**7, *1150*, 8-20, http://dx.doi.org/10.1016/j.molstruc.2017.08.068.
39. Chain, F.; Ladetto, M.F.; Grau, A.; Catalán, C.A.N.; Brandán, S.A. Structural, electronic, topological and vibrational properties of a series of N-benzylamides derived from Maca (*Lepidium meyenii*) combining spectroscopic studies with ONION calculations. *J. Mol. Struct*. **2016**, *1105*, 403-414, http://dx.doi.org/10.1016/j.molstruc.2015.10.082.
40. Chain, F.; Romano, E.; Leyton, P.; Paipa, C.; Catalán, C.A.N.; Fortuna, M.A.; Brandán, S.A. An experimental study of the structural and vibrational properties of sesquiterpene lactone cnicin using FT-IR, FT-Raman, UV–visible and NMR spectroscopies. *J. Mol. Struct*. **2014**, *1065-1066*, 160-169, http://dx.doi.org/10.1016/j.molstruc.2014.02.057.
41. Minteguiaga, M.; Dellacassa, E.; Iramain, M.A.; Catalán, C.A.N.; Brandán, S.A. Synthesis, spectroscopic characterization and structural study of 2-isopropenyl-3-methylphenol, carquejiphenol, a carquejol derivative with potential medicinal use. *J Mol. Struct*. **2018**, *1165*, 332-343, https://doi.org/10.1016/j.molstruc.2018.04.001.
42. Keresztury, G.; Holly, S.; Besenyei, G.; Varga, J.; Wang, A.Y.; Durig, J.R. Vibrational spectra of monothiocarbamates-II. IR and Raman spectra, vibrational assignment, conformational analysis and ab initio calculations of **S**-methyl-N,N-dimethylthiocarbamate. *Spectrochim. Acta* **1993**, *49A*, 2007-2026, https://doi.org/10.1016/S0584-8539(09)91012-1.
43. Michalska, D.; Wysokinski. The prediction of Raman spectra of platinum(II) anticancer drugs by density functional theory. *Chemical Physics Letters* **2005**, *403*, 211-217, https://doi.org/10.1016/j.cplett.2004.12.096
44. Besler, B.H.; Merz, Jr. K.M.; Kollman, P.A. Atomic charges derived from semiempirical methods. *J. Comp. Chem.* **1990**, *11*, 431-439, https://doi.org/10.1002/jcc.540110404.
45. Glendening, E.; Badenhoop, J.K.; Reed, A.D.; Carpenter, J.E.; Weinhold, F. NBO 3.1; *Theoretical Chemistry Institute, University of Wisconsin; Madison*, WI, 1996.
46. Bader, R.F.W. *Atoms in Molecules, A Quantum Theory*. Oxford University Press, Oxford, 1990.
47. Biegler-Köning, F.; Schönbohm, J.; Bayles, D. AIM2000; A Program to Analyze and Visualize Atoms in Molecules.

J. Comput. Chem. **2001**, *22*, 545, http://dx.doi.org/10.1002/1096-987X(20010415)22:5%3C545::AID-JCC1027%3E3.0.CO;2-Y.
48. Brandán, S.A. Why morphine is a molecule chemically powerful. Their comparison with cocaine. *Indian Journal of Applied Research* **2017**, *7*, 511-528.
49. Rudyk, R.A.; Brandán, S.A. Force field, internal coordinates and vibrational study of alkaloid tropane hydrochloride by using their infrared spectrum and DFT calculations. *Paripex A Indian Journal of Research* **2017**, *6*, 616-623.
50. Romani, D.; Brandán, S.A. Vibrational analyses of alkaloid cocaine as free base, cationic and hydrochloride species based on their internal coordinates and force fields. *Paripex A Indian Journal of Research* **2017**, *6*, 587-602.
51. Iramain, M.A.; Ledesma, A.E.; Brandán, S.A. Analyzing the effects of halogen on properties of a halogenated series of R and S enantiomers analogues alkaloid cocaine-X, X=F, Cl, Br, I. *Paripex A Indian Journal of Research* **201**7, *6*, 454-463.
52. Brandán, S.A. Understanding the potency of heroin against to morphine and cocaine. *International Journal of Science and Research Methodology* **2018**, *12*, 97-140.
53. Rudyk, R.A.; Checa, M.A.; Guzzetti, K.A.; Iramain, M.A.; Brandán, S.A. Behaviour of N-CH_3 Group in Tropane Alkaloids and correlations in their Properties. *International Journal of Science And Research Methodology* **2018**, *10*, 70-97.
54. Rudyk, R.A.; Checa, M.A.; Catalán, C.A.N.; Brandán, S.A. Structural, FT-IR, FT-Raman and ECD spectroscopic studies of free base, cationic and hydrobromide species of scopolamine alkaloid. *J. Mol. Struct.* **2018**, *1180*, 603-617.
55. Iramain, M.A.; Brandán, S.A. Structural and vibrational properties of three species of anti-histaminic diphenhydramine by using DFT calculations and the SQM approach. *Journal: To Chemistry Journal* **2018**, *1*, 105-130.
56. Márquez, M.J.; Iramain, M.A; Brandán, S.A. *Ab-initio* and Vibrational studies on Free Base, Cationic and Hydrochloride Species Derived from Antihistaminic Cyclizine agent. *International Journal of Science and Research Methodology* **2018**, *12*, 97-140.
57. Manzur, M.E.; Brandán, S.A. S(-) and R(+) Species Derived from Antihistaminic Promethazine Agent: Structural and Vibrational Studies. *Heliyon* **2019**, *5*, e02322, https://doi.org/10.1016/j.heliyon.2019.e02322.
58. https://spectrabase.com/spectrum/

6. ACKNOWLEDGEMENTS

This work was supported with grants from CIUNT Project Nº 26/D608 (Consejo de Investigaciones, Universidad Nacional de Tucumán, Argentina). The author would like to thank Prof. Tom Sundius for his permission to use MOLVIB.